



ELSEVIER

Contents lists available at ScienceDirect

## Journal of Pharmaceutical Sciences

journal homepage: [www.jpharmsci.org](http://www.jpharmsci.org)

Pharmaceutics, Drug Delivery and Pharmaceutical Technology

## Hot Melt Extrudates Formulated Using Design Space: One Simple Process for Both Palatability and Dissolution Rate Improvement



Lorena F.B. Malaquias<sup>1</sup>, Heidi L. Schulte<sup>1</sup>, Juliano A. Chaker<sup>2</sup>, Kapish Karan<sup>3</sup>, Thomas Durig<sup>3</sup>, Ricardo N. Marreto<sup>4</sup>, Tais Gratieri<sup>1</sup>, Guilherme M. Gelfuso<sup>1</sup>, Marcilio Cunha-Filho<sup>1,\*</sup>

<sup>1</sup> Laboratory of Food, Drug and Cosmetics (LTMAC), School of Health Sciences, University of Brasília, 70910-900 Brasília, Federal District, Brazil

<sup>2</sup> Faculty of Ceilândia, University of Brasília (UnB), 72220-900 Ceilândia, Federal District, Brazil

<sup>3</sup> Ashland Pharma and Nutrition, 500 Hercules Road, Wilmington, Delaware 19808

<sup>4</sup> School of Pharmacy, Federal University of Goiás, 74 605-170 Goiânia, Goiás, Brazil

## ARTICLE INFO

## Article history:

Received 24 July 2017

Revised 12 August 2017

Accepted 17 August 2017

Available online 26 August 2017

## Keywords:

dissolution rate

e-tongue

hot melt extrusion

hydrophilic polymers

itraconazole

palatability

## ABSTRACT

This work aimed at obtaining an optimized itraconazole (ITZ) solid oral formulation in terms of palatability and dissolution rate by combining different polymers using hot melt extrusion (HME), according to a simplex centroid mixture design. For this, the polymers Plasdione<sup>®</sup> (poly(1-vinylpyrrolidone-co-vinyl acetate) [PVP/VA]), Klucel<sup>®</sup> ELF (2-hydroxypropyl ether cellulose [HPC]), and Soluplus<sup>®</sup> (SOL, polyvinyl caprolactam-polyvinyl acetate-polyethylene glycol) were processed using a laboratory HME equipment operating without recirculation at constant temperature. Samples were characterized by physicochemical assays, as well as dissolution rate and palatability using an e-tongue. All materials became homogeneous and dense after HME processing. Thermal and structural analyses demonstrated drug amorphization, whereas IR spectroscopy evidenced drug stability and drug-excipient interactions in HME systems. Extrudates presented a significant increase in dissolution rate compared to ITZ raw material, mainly with formulations containing PVP/VA and HPC. A pronounced improvement in taste masking was also identified for HME systems, especially in those containing higher amounts of SOL and HPC. Data showed polymers act synergistically favoring formulation functional properties. Predicted best formulation should contain ITZ 25.0%, SOL 33.2%, HPC 28.9%, and PVP/VA 12.9% (w/w). Optimized response considering dissolution rate and palatability reinforces the benefit of polymer combinations.

© 2018 American Pharmacists Association<sup>®</sup>. Published by Elsevier Inc. All rights reserved.

## Introduction

Advantages of oral solid formulations are clear: high stability, dose accuracy, low production, and transportation costs, besides patient compliance.<sup>1</sup> Still, unsatisfactory physicochemical properties may compromise drug bioavailability. It is estimated that 75% of drug candidates to give rise to new medicines are poorly water soluble.<sup>2</sup> Such low solubility negatively affects pharmacokinetics, causing high rates of failure in clinical trials, which has considerably reduced the number of innovative medicines that reaches the market over the years.<sup>3</sup> Other challenge for oral delivery is the unpleasant taste of drugs, which adversely influences patient compliance, especially when dealing with children and elderly.<sup>4</sup> Most active pharmaceutical ingredients present bitter taste. Thus,

considering the wide variety of bitter receptors on the tongue, camouflaging drugs unpleasant taste is not a trivial task.<sup>5</sup>

Hot melt extrusion (HME) is a technological process for developing solid dispersions that has been capable of improving dissolution rates of many poorly water-soluble drugs.<sup>6,7</sup> Remarkable advantages of this technique include avoidance of organic solvents, possibility of continuous manufacturing, easy processing scale-up, and extrudate uniformity due to the high shear mixing capacity. Indeed, such a high mixing capacity provides a high drug-polymer interaction degree and, with the adequate formulation, bitter taste can be masked as polymers interact with tongue taste receptors masking the drug.<sup>5</sup>

Despite all these advantages, a still limited number of HME pharmaceutical products are available on the market, around 15 products.<sup>8</sup> A possible explanation is the complexity of experimental variables involved in the development of products by HME, which may compromise overall process robustness (mainly, the use of different temperatures throughout extrusion course and sample residence time into the system). Additionally, small fluctuations in

\* Correspondence to: Marcilio Cunha-Filho (Telephone/Fax: +55-61-31071990).

E-mail address: [marciliofarm@hotmail.com](mailto:marciliofarm@hotmail.com) (M. Cunha-Filho).

formulation composition can cause important changes in their properties. Evidently, all these factors raise quality issues, especially in large-scale production.<sup>9</sup>

Quality-by-design tools such as mixture designs are useful to rationalize the experimental work in order to establish the optimum formulation composition by determining a design space in which the components can fluctuate without impairing their functional characteristics, thus facilitating the scale-up process. Better yet, such approach also allows finding regions in the experimental space where the levels of formulation factors possibly provide the best performance.<sup>10</sup>

Therefore, this work evaluated a simplex centroid mixture design experiment as a tool for predicting the best polymer combination for HME of a bitter insoluble drug. The goal was to obtain the best formulation for HME with improved characteristics, specifically, palatability and dissolution rate, by simply selecting the better suited excipients, while maintaining the most simple process parameters: constant temperature and no recirculation. For this, itraconazole (ITZ) was selected as drug model, because it is a BCS II compound possessing a pronounced bitter taste and promising results when processed by HME.<sup>11-14</sup> The hydrophilic polymers Plasdone® S-630, Klucel® ELF, and Soluplus® were chosen to improve drug dissolution through different solubilization mechanisms.

## Experimental

### Material

ITZ (lot 00569488, 99.5%) was provided by Roche (Basel, Switzerland). The polymers Plasdone S-630 (lot 0001810863, poly(1-vinylpyrrolidone-co-vinyl acetate) [PVP/VA], average molecular weight = 47 kDa) and Klucel ELF (lot 40915, 2-hydroxypropyl ether cellulose [HPC], average molecular weight = 40 kDa) were donated by Ashland Specialty Ingredients, whereas Soluplus ([SOL] lot 844143368EO, polyvinyl caprolactam-polyvinyl acetate-polyethylene glycol, average molecular weight = 118 kDa) was donated by BASF (Ludwigshafen, Germany). All other chemicals and solvents were of analytical grade.

### HME Extrudates

Extrudates were prepared by HME combining ITZ with 3 polymers (PVP/VA, HPC, and SOL) following a simplex centroid mixture design without constraints (in detail in section [Design of Experiment](#)). For this, ITZ concentration was fixed at 25% w/w in each sample ([Table 1](#)). Physical mixtures of each formulation were prepared using a mortar and were then extruded using constant temperature without sample recirculation in a Pharma Mini HME (ThermoScientific). Extrusion parameters, temperature and rotation speed, were set with the purpose of obtaining an adequate extrusion flow and translucent extrudates without darkening ([Table 1](#)). Extrudates were milled in a knife mill and the fractions were separated using sieves with different mesh. After separation, a powder fraction having a size ranging from 180 to 125 μm, which was the fraction with the best yield, was selected for further tests.

### Characterization Assays

#### Drug Determination

A spectrophotometric method using a UV-VIS Lambda XLS spectrophotometer (PerkinElmer) set at 255 nm was developed for ITZ determination in formulations and in dissolution rate experiments. Analytical method was validated. Selectivity against polymers was evaluated and no statistical interference with excipients was detected (Student t-test,  $p = 0.07$ ). Linearity correlation coefficient (CC) was 0.9984 with slope different from zero and residues randomly distributed without tendency.

#### Morphological Analysis

Morphological characteristics of the individual compounds, physical mixtures, and extrudates were assessed with a stereoscope (Laborana/SZ—SZT, China) and with a scanning electron microscope (JSM-7001F; Jeol, Akishima, Japan), in which the samples were previously metallized with gold.

**Table 1**  
Summary of the Formulation Compositions and the Extrusion Parameters

Formulation	Composition (% w/w)			Temperature (°C)	Rotation (rpm)	Design Representation
	SOL	HPC	PVP/VA			
FA	75	0	0	170	50	
FB	0	75	0	170	50	
FC	0	0	75	170	100	
FD	37.5	37.5	0	170	50	
FE	0	37.5	37.5	170	50	
FF	37.5	0	37.5	170	50	
FG	25	25	25	170	50	

### Thermal Properties

Differential scanning calorimetry (DSC) curves were obtained from a DSC-60 (Shimadzu, Kyoto, Japan). Approximately 3 mg of each sample was placed in aluminum-sealed pans and analyzed under nitrogen atmosphere (flow rate of 50 mL/min) at a heating rate of 10°C/min from 30°C to 300°C. Tests were performed on individual compounds, physical mixtures, and extrudates. ITZ original crystalline form percentage (%OCF) in the HME systems was calculated based on melting enthalpy following the equation:

$$\%OCF = (\Delta H_{HME} / \Delta H_{ITZ}) \times 100$$

where  $\Delta H_{HME}$  is the fusion enthalpy of ITZ in HME system and  $\Delta H_{ITZ}$  is the fusion enthalpy of ITZ raw material.

### Molecular Studies

The FTIR spectra were recorded on an IRAffinity-1SFTIR spectrophotometer (Shimadzu) between 4000 and 400  $\text{cm}^{-1}$  at an optical resolution of 4.0  $\text{cm}^{-1}$ , totaling an average of 40 scans. Tests were carried out on individual compounds, physical mixtures, and extrudates recorded with crystalline KBr. CC between physical mixtures and HME systems was calculated using an Essential FTIR<sup>®</sup> software (EUA).<sup>15</sup> A peak deconvolution analyses of ITZ C–H stretch envelop in the range 3050 to 2750  $\text{cm}^{-1}$  were performed using PeakFit 4.0 software considering pseudo-Voigt single shaped absorption bands.<sup>16</sup>

### Structural Analyses

X-ray powder diffraction (XRPD) analysis was performed using a Miniflex diffractometer 600 (Rigaku, Tokyo, Japan) equipped with a high-speed scintillation detector and a graphite monochromator ( $\lambda = 1.5418 \text{ \AA}$ ). Diffraction patterns were obtained at angles between  $-5^\circ$  and  $60^\circ$  ( $\theta - 2\theta$ ). Tests were carried out on the individual compounds, physical mixtures, and extrudates.

### Dissolution Test

ITZ dissolution profiles were obtained for raw material and extrudates in a dissolutor Ethik model 299 (Brazil) using 900 mL of HCl 0.1 mol/L maintained at 37°C, and apparatus 2 (paddle) operating at 75 rpm.<sup>17</sup> Samples of 5 mL were withdrawn and immediately replaced by fresh dissolution medium at 5, 10, 15, 20, 30, 45, 60, 90, and 120 min. After filtration through 0.45- $\mu\text{m}$  membranes (PES Millipore, Beijing, China), samples were diluted 1:5 (v/v) with HCl 0.1 mol/L and taken to spectrophotometer for ITZ content quantification following the method described in the section **Drug Determination**. Experiments were performed in quadruplicate using samples containing the equivalent to 100 mg ITZ.

Dissolution profiles were evaluated using dissolution efficiency at 30 min (DE<sub>30</sub>).<sup>18</sup> Data were analyzed by 1-way ANOVA followed by Tukey post-test using IBM SPSS Statistics 22 version. Significance level was fixed at 0.05. Normality of data were tested and showed parametric behavior.

### In Vitro Taste-Masking Evaluation (Astree E-tongue)

The taste masking provided by the formulations was evaluated applying the Astree e-tongue system equipped with an Alpha M.O.S sensor set #2 composed by 7 sensors, that is, ZZ, AB, GA, BB, CA, DA, and JE (Alpha M.O.S, Toulouse, France). The software reduces the data received from the 7 sensors using multivariate statistic algorithms. For all samples, the individual principle components with more information (PC1 and PC2) were used to create a 2-dimensional map, namely principal component analysis (PCA). The assay was performed using equivalent amounts of 100 mg ITZ of each extrudate dispersed into 50 mL of distilled water, gently shaken for 30 s and filtered using fiber glass of 1  $\mu\text{m}$ . Acquisition times were set at 120 s at 25°C. Ten replicates were measured and

the average values between 100 and 120 s were used to build a 2-dimensional map (PCA). Relative SD was computed for measuring replicates of a single sample for each sensor. Based on the repeatability of measurement (relative standard deviation = 0.47 to 1.51), the method was considered fitted for the study.<sup>19</sup> Distances between extrudates and placebo and between extrudates and unprocessed drug were calculated as indicative of formulation taste-masking power.

### Design of Experiment

Responses from dissolution profile (DE<sub>30</sub>) assays and taste-masking evaluation (distance from placebo) were modeled according to a simplex centroid mixture design, in which the selected polymers were combined as described in Table 1.<sup>20</sup> The best fitting mathematical model was selected for each response. Specifically, results were fitted using polynomial functions of PVP/VA, HPC, and SOL contents with stepwise multiple regression analyses. Model validation was performed using ANOVA and coefficients of determination ( $r^2$ ) at  $p < 0.05$ .<sup>20</sup> An additional response surface from both responses was built considering the formulation conditions to maximize dissolution and palatability properties of ITZ HME (optimized response), in which the 2 responses were adjusted with the same importance. The optimized response was calculated from the geometric mean. All calculations and the contour diagrams were drawn using Design-Expert<sup>®</sup> Software version 8.

## Results and Discussion

### Characterization Assays

Processing temperature used to obtain the extrudates was 170°C, which is above ITZ melting peak (168°C) and glass transition of the polymers (130°C, 110°C, and 70°C for HPC, PVP/VA, and SOL, respectively), providing the proper miscibility between drug and polymers. All samples demonstrated in these conditions appropriate extrusion behavior with continuous flow, drug content (assay > 90%), and uniformity (0.1%  $\leq$  SD  $\leq$  1.9%; Table 2).

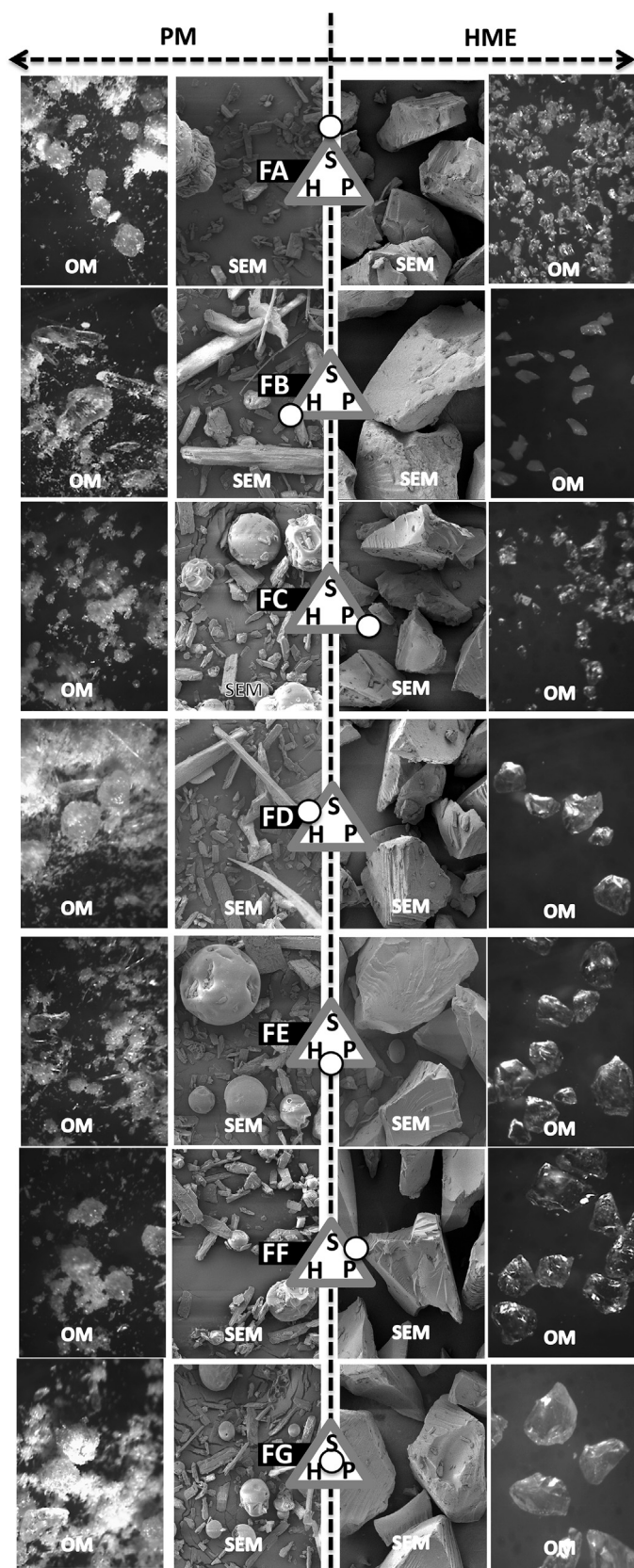
Systems containing HPC showed translucent aspect as soon as they left the equipment die, but became opaque few seconds later, suggesting drug recrystallization, except for quaternary system (FG), which had a reduced amount of HPC (25% w/w) and preserved the translucent aspect after cooling. All other samples exhibited a translucent aspect (Table 2).

Figure 1 presents the microscopical aspects of physical mixtures and HME formulations. In physical mixtures, each component can be individually identified (the crystalline ITZ and amorphous polymers), whereas in HME systems only one phase is observed. HME process generated homogeneous products with a considerable change in samples aspect, suggesting the drug is immersed into the polymer in a high level of dispersion. The opaque aspect of the HPC system (FB) is noticed as a binary system, contrasting with the translucent aspect of others extrudates. All extrudates showed a dense aspect without pores (Fig. 1).

**Table 2**  
Aspect and Drug Content of the Formulations

Formulation	Aspect	Drug Content (% w/w $\pm$ SD)
FA	Slightly yellowish and translucent	103.0 $\pm$ 1.9
FB	Opaque	90.3 $\pm$ 0.4
FC	Slightly yellowish and translucent	103.5 $\pm$ 0.4
FD	Slightly opaque	100.9 $\pm$ 0.5
FE	Slightly opaque	104.6 $\pm$ 0.4
FF	Slightly yellowish and translucent	93.1 $\pm$ 0.3
FG	Slightly yellowish and translucent	99.0 $\pm$ 0.1





**Figure 1.** Optical microscopy (25 $\times$ ) and scanning electron microscope (30 $\times$ ) micrographs of physical mixtures and HME systems (FA, FB, FC, FD, FE, FF, and FG).

Following thermal analysis, ITZ raw material and all physical mixtures generated an endothermic peak at 168 $^{\circ}$ C, which corresponds to the drug melting.<sup>21</sup> This peak was vanished for the majority of extrudates, indicating the disappearance of the original crystalline form (Fig. 2). Nevertheless, in the binary and ternary systems with HPC (FB and FD), ITZ melting peak remained detectable, presenting a minor shift to a lower temperature and a marked reduction in the expected enthalpy. Crystallinity degrees of these samples were 35.6% and 8.0%, respectively (Fig. 2). Thermal profiles of FB and FD support morphological results, denoting the presence of crystalline material in these samples.

Diffractograms of ITZ raw material, polymers, and extrudates are shown in Figure 3. ITZ presented a typical crystalline profile whereas polymers assumed an amorphous behavior. All HME formulations, including formulations FB and FD, displayed a completely amorphous XRPD profile, which would indicate a high amount of drug in the amorphous form. Considering, however, that DSC can be more sensitive and specific than XRPD in determining drug/excipient interactions, once minor disturbances at drug-excipient interface causes detectable changes in thermal events of the samples,<sup>22,23</sup> it may be assumed ITZ is solubilized into the polymers in a molecular level after HME processing, except in the binary and ternary systems with HPC, namely FB and FD.

CC of FTIR spectra was calculated comparing HME systems and its physical mixtures and, except for formulation FB, all samples demonstrated CC above 0.85, which indicated no significantly destructive interaction.<sup>15</sup> For formulation FB, however, CC value was 0.70. Spectral differences can be observed between samples with different drug homogeneity.<sup>24</sup> Morphological analysis has already suggested a decrease in matrix homogeneity in FB, which can explain the lower CC value observed for this formulation. Besides, the FB extrudate preserved all functional groups of the drug and the polymer, which demonstrates the stability of this sample.

Polymer-drug interactions were investigated based on C–H band absorption of ITZ in the range of 3050 to 2750  $\text{cm}^{-1}$ . C–H absorption assignments involved in hydrophilic sites of ITZ as well as absorption peak assignments associated with hydrophobic sites of ITZ are shown in Figure 4.<sup>25</sup> The sum of absorption peak areas from hydrophilic ITZ region decreased at the following order: FB > FE > FD > FG > FF > FA > FC. Opposite behavior was observed from hydrophobic ITZ region, which obeyed the following sequence: FC > FF > FG > FA > FD > FE > FB.

Results indicated the drug interacted with each polymer in a different manner. The most hydrophilic polymer, HPC, caused strong absorption intensity in ITZ hydrophilic sites and weak absorption intensity on drug hydrophobic sites. This behavior contrasted to that found for PVP/VA samples, which presented weak absorption intensities for ITZ hydrophilic sites and high absorption intensities for hydrophobic sites. SOL, in its turn, appeared to interact less intensively with ITZ. Because the intensity of IR is mainly governed by the dipole moment of absorbing bond,<sup>26</sup> it is plausible to assume the increase in absorption intensity is a result of a dipole enhancement caused by ITZ and the different polymer interactions.

Moreover, the peak belonging to C–O–C stretch (ether group, 1203  $\text{cm}^{-1}$ ) was weakly detected in physical mixtures of formulations FC, FE, and FF and was completely absent in their respective HME samples. Such systems have PVP/VA in common, which has already reported to produce H-bonding interactions with other drugs in solid dispersions produced by HME.<sup>27</sup> These interactions may favor the drug miscibility, improving the translucent aspect observed in samples with PVP/VA in binary system. No other changes regarding the stretches of polymer bonding were noted.

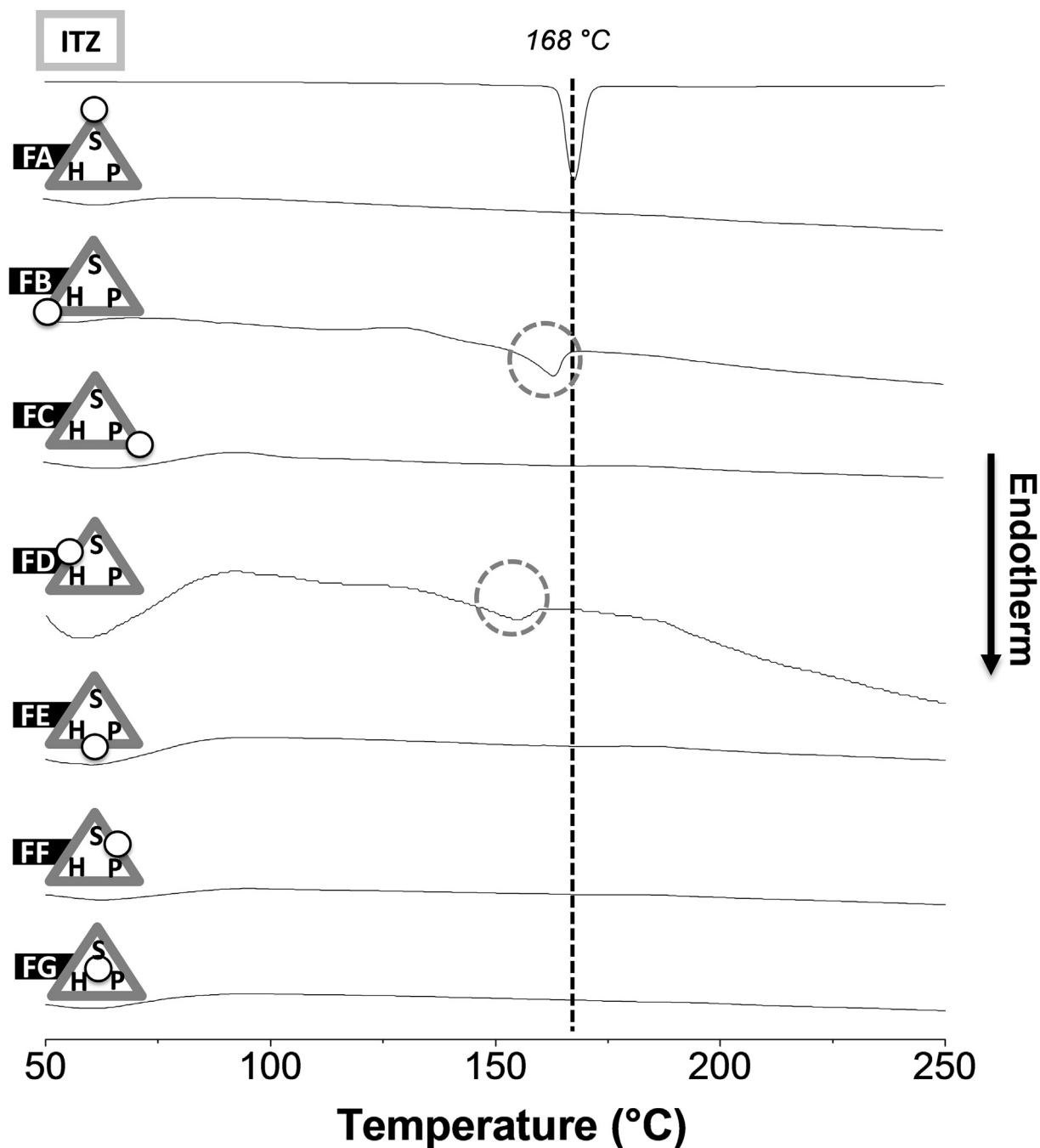


**Figure 2.** DSC analysis of ITZ raw material and HME systems (FA, FB, FC, FD, FE, FF, and FG). Drug melting peak is highlighted.

#### Dissolution Tests

HME process was capable of improving ITZ dissolution rate, being more than 80% of the drug dissolved in 30 min versus around 5% of ITZ raw material dissolved over the same period of time (Fig. 5). Formulations FG and FF presented an outstanding performance with  $DE_{30}$  around 90%, distinguishing from the other formulations. FA showed the slowest drug dissolution profile with a  $DE_{30}$  of 59%, but still far superior to ITZ as supplied ( $DE_{30} = 1.3\%$ ). The inferior dissolution rate of FA can be correlated to the lower degree of drug-polymer interaction observed by FTIR. No significant differences in drug dissolution were identified among formulations FB, FC, FD, and FE.

The experimental mixture design performed led to a predictive equation for ITZ  $DE_{30}$  using a special cubic mathematical approach (Table 3). The model was validated by ANOVA, multiple CC, and lack of fit. All predictive equation terms showed  $p < 0.05$ , except PVP/VA:HPC which exhibited  $p = 0.77$ . According to this equation, the positive signs of the terms refer to an increase in  $DE_{30}$ , and the magnitude of the coefficients indicates the contribution of each component of the mixture to this response.

The fitted model for  $DE_{30}$  showed a positive contribution of all polymers and a significant interaction within their combination (Table 3). Individually, PVP/VA and HPC improved ITZ dissolution, showing higher coefficients than SOL. Relevant interactions between SOL and each of the other 2 polymers

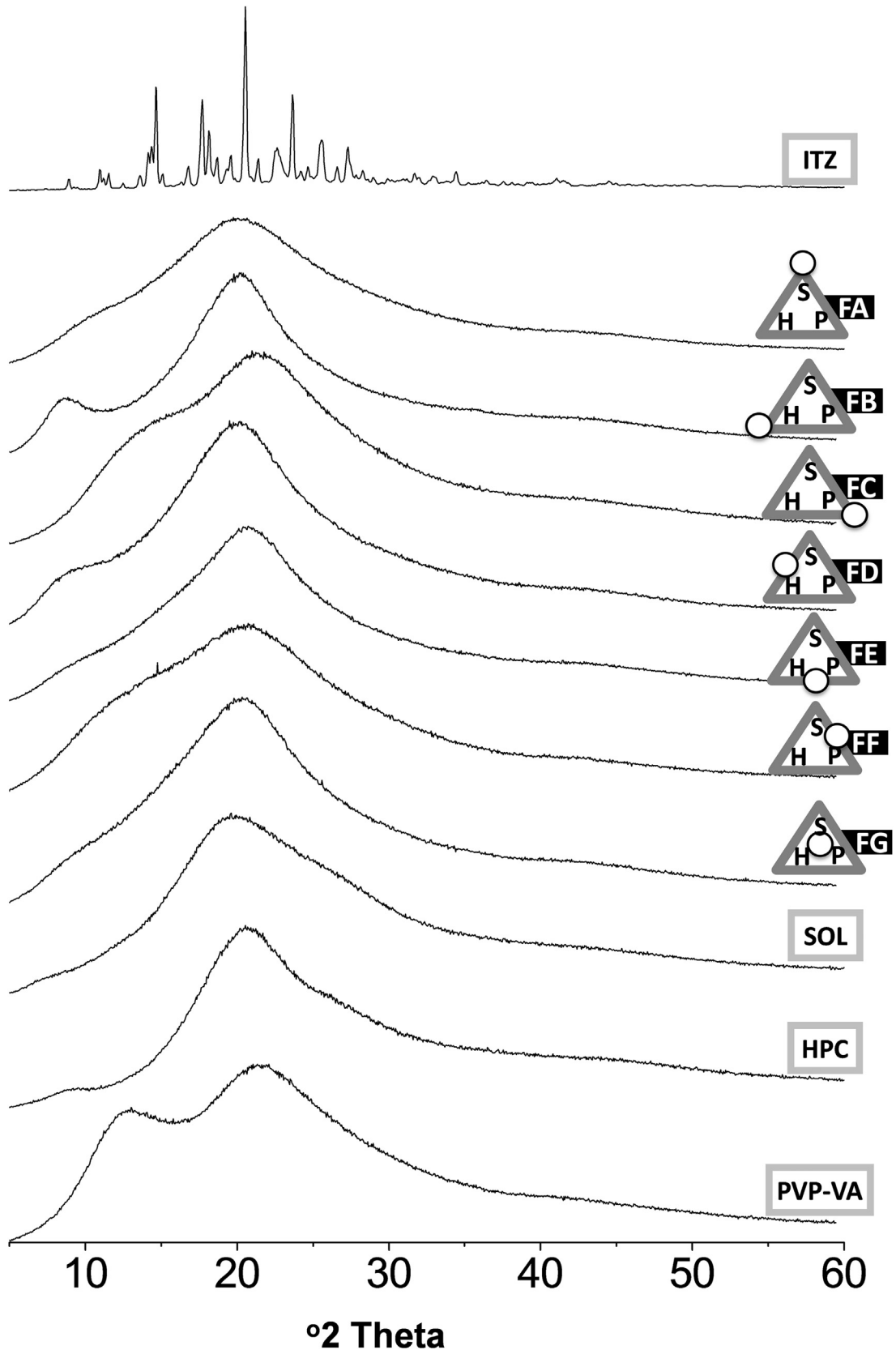
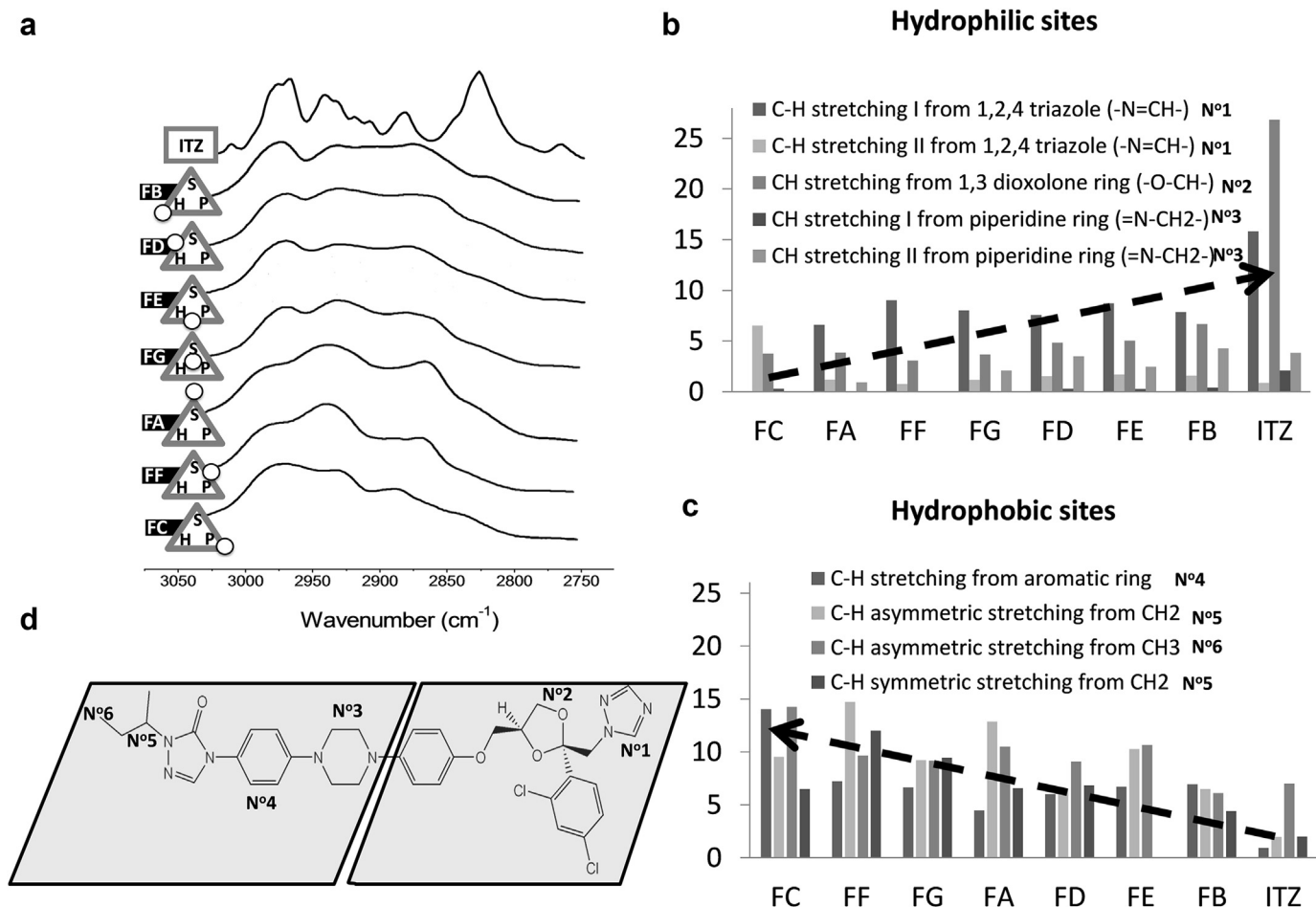


Figure 3. XRPD patterns of ITZ and polymers as supplied, and HME systems (FA, FB, FC, FD, FE, FF, and FG).



**Figure 4.** FTIR fitting simulation obtained from experimental data of the ITZ absorption C–H bands in the range 3050 to 2750  $\text{cm}^{-1}$  for ITZ raw material and HME systems (FA, FB, FC, FD, FE, FF, and FG) (a). The proportional areas of each peak from hydrophilic sites of ITZ (b), namely 1,2,4 triazole (N° 1), 1,3 dioxolone (N° 2), and piperidine ring (N° 3); and from hydrophobic sites of ITZ (c), namely C–H stretching from aromatic ring (N° 4), asymmetrical and symmetrical stretching from CH<sub>2</sub> (N° 5) and asymmetrical stretching from CH<sub>3</sub> (N° 6), were assigned in the ITZ molecule (d).

potentiated the ITZ dissolution. Still, when the 3 components were mixed with ITZ, dissolution was also improved, as it can be seen by the high coefficient of this factor, demonstrating a relevant synergistic contribution of each polymer in the dissolution of the drug.

A contour diagram was drawn using the refined model as shown in Figure 6. The darker areas represent the formulation compositions that produced the best DE<sub>30</sub> results. The darker areas of the graphic occur in the center, where there is a more equivalent distribution of the 3 polymers. Good dissolution results were also achieved close to the vertices of the diagram containing PVP/VA and HPC polymers, which show these materials, individually, significantly contribute to the ITZ dissolution.

Differences in drug-exipient interaction based on polymer characteristics as pointed out by FTIR spectra may be the starting point to explaining extrudate differences in dissolution performance but certainly should not be the only one. Because drug is mostly or totally in amorphous state, ITZ release from HME systems will strongly depend on the polymers' solubilization mechanisms. PVP/VA and HPC produce hydrophilic matrices that are rapidly solubilized and erode as soon the wetting starts, whereas SOL matrices undergo a gradual formation of a surface gel layer in which the drug diffuses.<sup>28</sup> Micellization is also reported as a solubilization mechanism of SOL.<sup>29</sup> In the present study, these different mechanisms act together to improve ITZ dissolution and may be

the reason why the combination of the polymers has led to a better drug dissolution.<sup>30</sup>

#### In Vitro Taste-Masking Evaluation

E-tongue sensors imitate taste bud on human tongue by initiating changes in electric potentials that can be compared to physiological action.<sup>31</sup> This *in vitro* assay presents a high correlation with human sensory test and is until 100 times more sensitive for bitter taste than human panel.<sup>32</sup> The electric potentials generated by the samples, which correspond to the physiological taste, are recorded by a computer system in a 2-dimensional chart containing the signal distances between the drug, formulations, and placebo. A successful taste masking is achieved when the formulation signals are far from drug and close to placebo.

According to the results presented in Figure 7, Astree e-tongue was capable of identifying taste difference between extrudates and unprocessed ITZ. Additionally, differences between the extrudates themselves were observed, which corroborates with the physicochemical findings. Based on the PCA chart (Fig. 7), no formulation completely masked ITZ taste, because there was no overlap of placebo and extrudates. Nevertheless, FA and FB HME are closer to placebo than the other formulations.

The predictive equation for distance from placebo was adjusted to a special cubic model in which all terms showed  $p < 0.05$



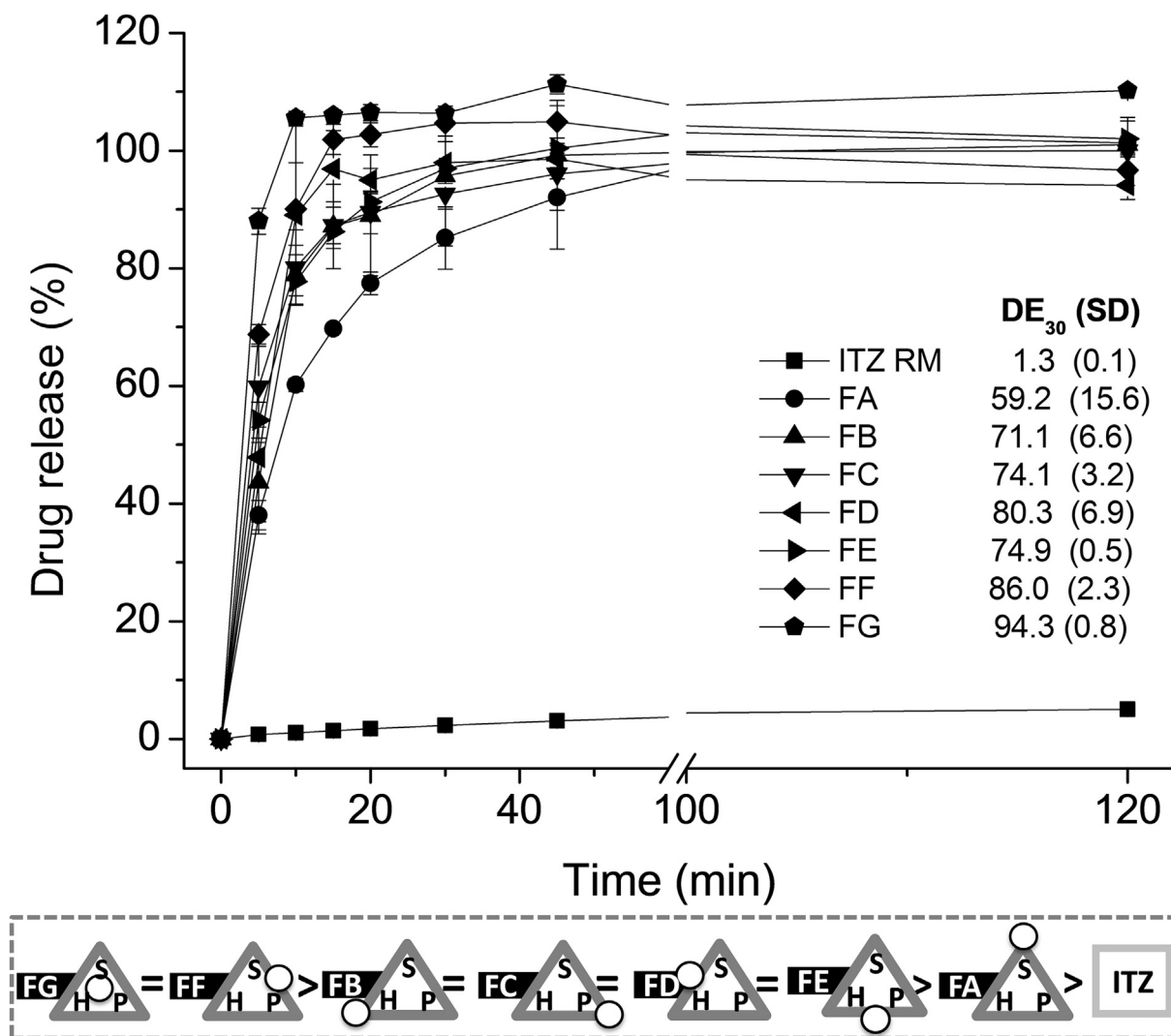


**Figure 5.** ITZ raw material dissolution profile compared with HME samples (FA, FB, FC, FD, FE, FF, and FG), together with the corresponding mean values of the DE<sub>30</sub> and the SD in parentheses. Significant DE<sub>30</sub> differences were identified among samples in the dashed square.

(Table 3). Contour diagram of formulation distance from the placebo are shown in Figure 6. Regions containing larger amounts of SOL and HPC (darker areas) presented significant improvement in palatability. Palatability improvement provided by formulations containing SOL has already been reported before.<sup>33</sup>

The taste-masking ability of extrudates could be related to drug dispersion into polymeric matrix and to sample dissolution behavior. Better results of taste masking achieved by HME systems containing SOL could be explained by the capacity of this polymer to form micelles, in which the drug is isolated inside the structure, less available to activate electric potential in Astree e-tongue.<sup>34</sup> Moreover, the ability of taste masking of FB extrudate could be related to the presence of drug in crystalline form, as suggested by

morphological characterization and thermal analysis, as well as to the high drug-polymer interaction as observed by FTIR analysis.

#### Prediction of the Optimized Formulation

Experimental designs are useful to reduce the development time of products. Ideal formulations can be predicted regarding a required performance using less experimental effort and appropriate statistical approach. In this sense, optimized response considering DE<sub>30</sub> and distance from placebo was calculated (Fig. 6). The gray area represents formulation compositions that maximize ITZ dissolution and palatability characteristics. Optimized response assumes values  $\geq 0.8$ .

**Table 3**

Mixture Design Statistical Parameters Including the Predictive Equation for the Model Based on DE<sub>30</sub> and Distance From Placebo Responses

Fitted Model	DE <sub>30</sub>	Distance from Placebo
	Special Cubic	Special Cubic
<i>p</i> Value	<0.0001	<0.0001
<i>r</i> <sup>2</sup>	0.84	0.99
Predictive equation	= + 56.3 SOL + 75.7 PVP/VA + 73.1 HPC + 82.4 SOL:PVP/VA + 57.3 SOL:HPC + 3.7 PVP/VA:HPC + 269.2 SOL:PVP/VA:HPC	= + 353 SOL + 390 PVP/VA + 313 HPC + 366 SOL:PVP/VA + 68 SOL:HPC + 982 PVP/VA:HPC - 2223 SOL:PVP/VA:HPC



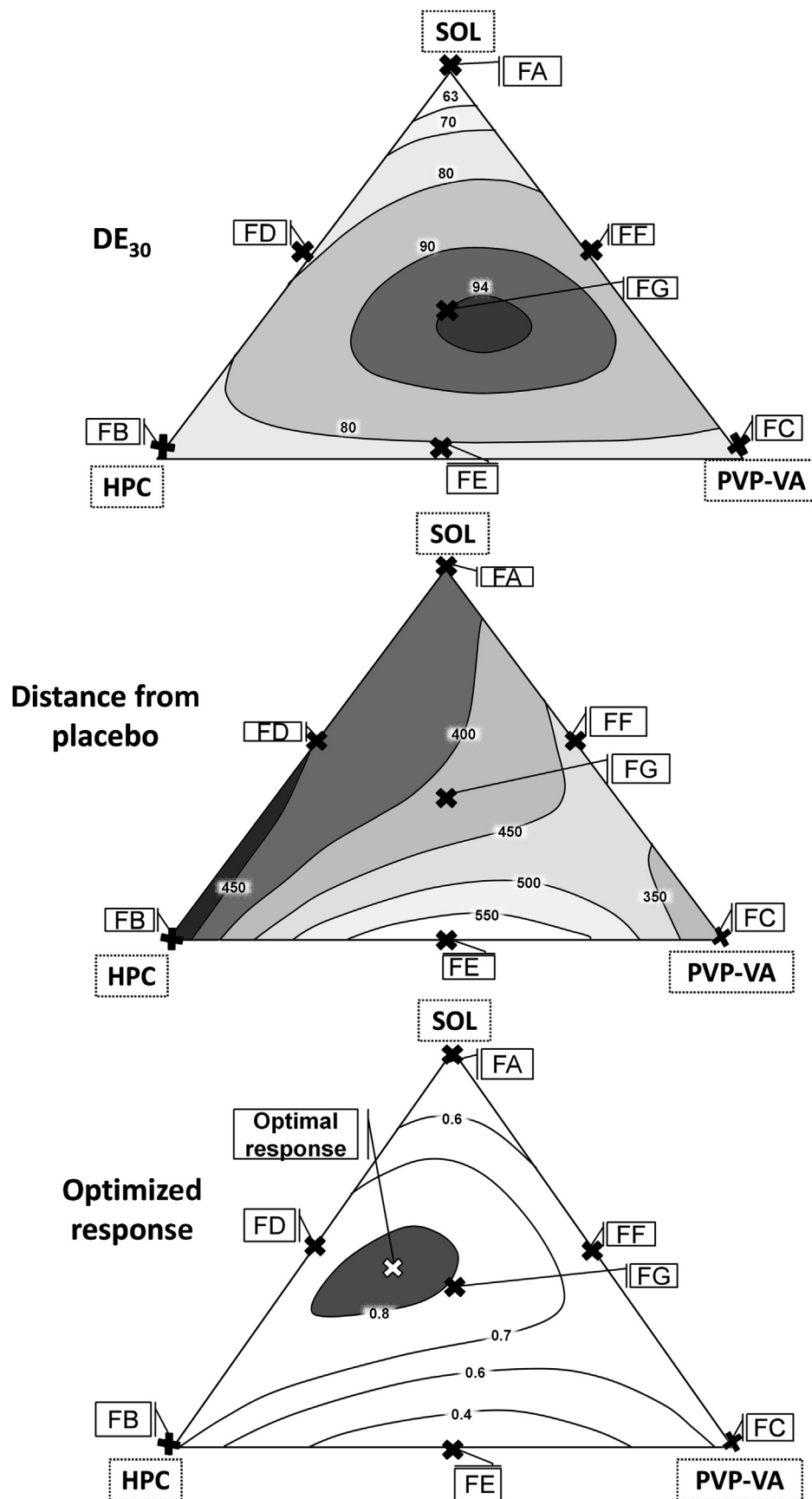


**Figure 6.** Contour diagrams for  $DE_{30}$  and distance from placebo. Experimental points are assigned and dark areas show the regions with better response. A contour diagram for the optimized response considering both  $DE_{30}$  and distance is shown.

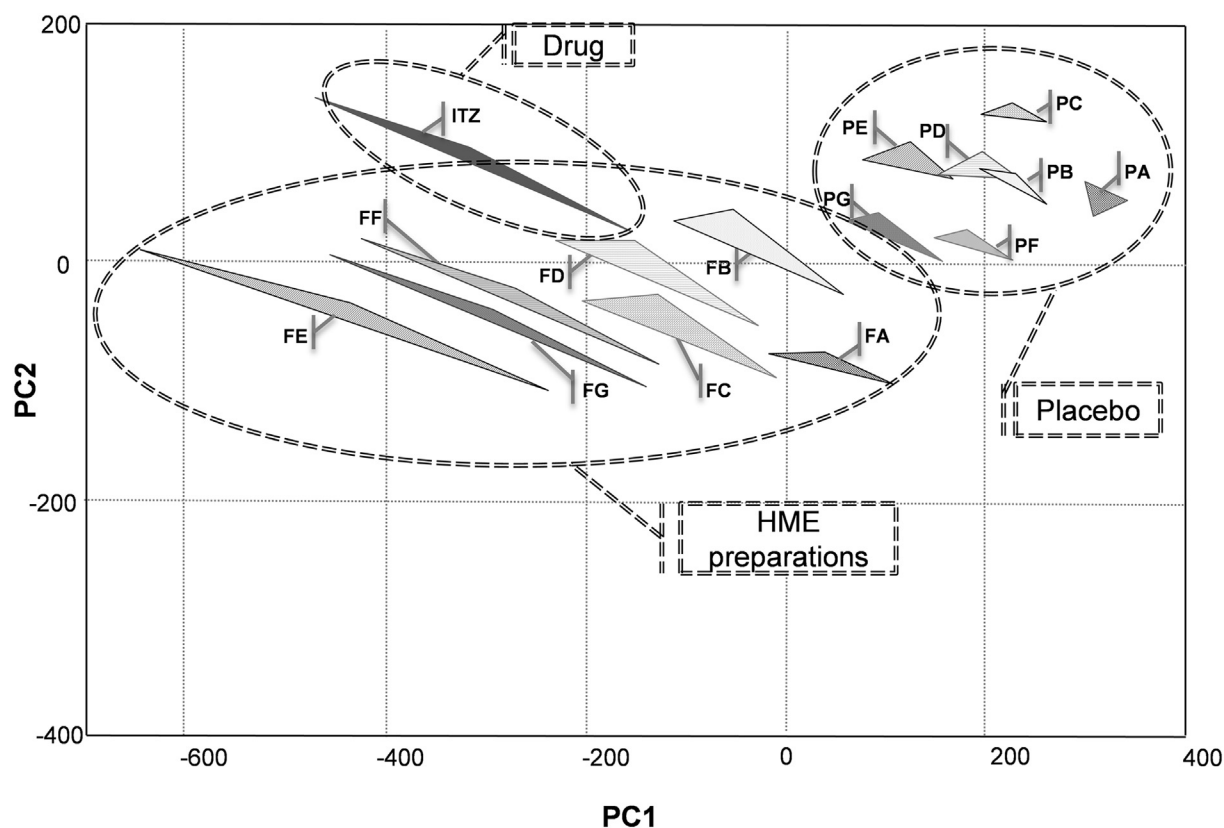


Figure 7. Two-dimensional PCA chart (PC1 and PC2) of taste-masking evaluation of HME extrudates using Astree e-tongue.

The diagram area highlighted in gray was close to the center, which corresponds to the presence of the 3 polymers in formulation, reinforcing the benefit of combining these materials. Within the limits of the gray area, polymer concentrations fluctuate interdependently. As a result, SOL can vary in the concentration range of 42% to 12% (w/w); HPC in the range of 43% to 20% (w/w); and PVP/VA can fluctuate from 6% up to 22% (w/w). Thus, predicted best formulation indicated in Figure 6 by the white X should contain the following composition (w/w): ITZ 25.0%, SOL 33.2%, HPC 28.9%, and PVP/VA 12.9%.

## Conclusion

The use of mixture design, allied with microscopy techniques, DSC, XRPD, and FTIR, identified drug-excipient interactions of solid mixtures composed of ITZ produced by HME using the polymers SOL, PVP/VA, and HPC. An optimum formulation composition could be selected for the model drug ITZ, which enhanced the drug dissolution rate and masked the bitter taste. This could be achieved using simple process parameters as constant temperature and single step without sample recirculation. Data obtained demonstrated proper experiment design might be useful in selecting the best excipient combination for a specific desired formulation performance.

## Acknowledgments

This research was supported by Brazilian agencies CNPq and CAPES. The authors would like to thank the valuable contribution of Daniela Galter and Karina Riccomini in the taste-masking studies.

## References

1. Fridgeirsdottir GA, Harris R, Fischer PM, Roberts CJ. Support tools in formulation development for poorly soluble drugs. *J Pharm Sci.* 2016;105:2260-2269.
2. Di L, Fish PV, Mano T. Bridging solubility between drug discovery and development. *Drug Discov Today.* 2012;17:486-495.
3. Mignani S, Huber S, Toma H. Compound high-quality criteria: a new vision to guide the development of drugs, current situation. *Drug Discov Today.* 2016;21:573-584.
4. Boateng J. Drug delivery innovations to address global health challenges for pediatric and geriatric populations (through improvements in patient compliance). *J Pharm Sci.* [Epub ahead of print] July 20, 2017.
5. Maniruzzaman M, Boateng JS, Bonnefille M, Aranyos A, Mitchell JC, Douroumis D. Taste masking of paracetamol by hot-melt extrusion: an in vitro and in vivo evaluation. *Eur J Pharm Biopharm.* 2012;80:433-442.
6. Rantanen J, Khinast J. The future of pharmaceutical manufacturing sciences. *J Pharm Sci.* 2015;104:3612-3638.
7. Patil H, Tiwari RV, Repka MA. Hot-melt extrusion: from theory to application in pharmaceutical formulation. *AAPS PharmSciTech.* 2015;17:20-42.
8. Tiwari RV, Patil H, Repka MA. Contribution of hot-melt extrusion technology to advance drug delivery in the 21st century. *Expert Opin Drug Deliv.* 2016;13:451-464.
9. Thiry J, Krier F, Evrard B. A review of pharmaceutical extrusion: critical process parameters and scaling up. *Int J Pharm.* 2015;479:227-240.
10. Carmo ACM, Cunha-Filho MSS, Gelfuso GM, Gratieri T. Evolution of quality on pharmaceutical design: regulatory requirement? *Accredit Qual Assur.* 2017;22:199-215.
11. Six K, Verreck G, Peeters J, Brewster M, Van Den Mooter G. Increased physical stability and improved dissolution properties of itraconazole, a class II drug, by solid dispersions that combine fast- and slow-dissolving polymers. *J Pharm Sci.* 2004;93:124-131.
12. Yamaguchi H, Dan K, Saito K, Kobayashi A, Kainuma M, Hasegawa S. The effects of dilution of itraconazole oral solution with distilled water or simple syrup on the pharmacokinetics property and on taste. *Jpn Pharmacol Ther.* 2009;37:307-314.
13. DiNunzio JC, Brough C, Miller DA, Williams III RO, McGinity JW. Fusion processing of itraconazole solid dispersions by kinetisol® dispersing: a comparative study to hot melt extrusion. *J Pharm Sci.* 2010;99:1239-1253.
14. Sarode AL, Sandhub H, Shahb N, Malick W, Zia H. Hot melt extrusion (HME) for amorphous solid dispersions: predictive tools for processing and impact of drug-polymer interactions on supersaturation. *Eur J Pharm Sci.* 2013;48:371-384.

15. Mecozzi M, Pietroletti M, Monakhova YB. FTIR spectroscopy supported by statistical techniques for the structural characterization of plastic debris in the marine environment: application to monitoring studies. *Mar Pollut Bull.* 2016;106:155-161.
16. Stuart B. *Infrared Spectroscopy: Fundamentals and Applications*. 1st ed. NJ: John Wiley & Sons; 2004:244.
17. Lang B, McGinity JW, Williams RO. Dissolution enhancement of itraconazole by hot-melt extrusion alone and the combination of hot-melt extrusion and rapid freezing-effect of formulation and processing variables. *Mol Pharm.* 2014;11:186-196.
18. Khan KA, Rhodes CT. The concept of dissolution efficiency. *J Pharm Pharmacol.* 1975;27:48-49.
19. Li X, Gao X, Liu R, et al. Optimization and validation of the protocol used to analyze the taste of traditional Chinese medicines using an electronic tongue. *Exp Ther Med.* 2016;12:2949-2957.
20. Alves-Silva I, Marreto RN, Gelfuso GM, Sá-Barreto LCL, Lima EM, Cunha-Filho MSS. Preparation of benzimidazole pellets for immediate drug delivery using the extrusion spheronization technique. *Drug Dev Ind Pharm.* 2016;43:762-769.
21. Alves-Silva I, Sá-Barreto LCL, Lima EM, Cunha-Filho MSS. Preformulation studies of itraconazole associated with benzimidazole and pharmaceutical excipients. *Thermochim Acta.* 2014;575:29-33.
22. Marini A, Berbenni V, Moiola S, et al. Drug excipient compatibility studies by physico-chemical techniques: the case of indomethacin. *J Therm Anal Calorim.* 2003;73:529-545.
23. Bruni G, Berbenni V, Milanese C, Girella A, Marini A. Drug-excipient compatibility studies in binary and ternary mixtures by physico-chemical techniques. *J Therm Anal Calorim.* 2010;102:193-201.
24. Feng X, Vo A, Patil H, et al. The effects of polymer carrier, hot melt extrusion process and downstream processing parameters on the moisture sorption properties of amorphous solid dispersions. *J Pharm Pharmacol.* 2016;68:692-704.
25. Murti Y, Agnihotri R, Pathak D. Synthesis, characterization and pharmacological screening of some substituted 1,2,3- & 1,2,4-triazoles. *Am J Chem.* 2011;1:42-46.
26. Goyal M, Prajapati N. Preparation and characterization of solid dispersion of itraconazole. *J Pharm Sci Innov.* 2013;2:23-28.
27. Forster A, Hempenstall J, Rades T. Characterization of glass solutions of poorly water-soluble drugs produced by melt extrusion with hydrophilic amorphous polymers. *J Pharm Pharmacol.* 2001;53:303-315.
28. Punčochová K, Ewing AV, Gajdošová M, et al. Identifying the mechanisms of drug release from amorphous solid dispersions using MRI and ATR-FTIR spectroscopic imaging. *Int J Pharm.* 2015;483:256-267.
29. Lavra ZMM, Pereira de Santana D, Ré MI. Solubility and dissolution performances of spray-dried solid dispersion of Efavirenz in Soluplus. *Drug Dev Ind Pharm.* 2016;9045:1-13.
30. Punčochová K, Ewing AV, Gajdosova M, et al. The combined use of imaging approaches to assess drug release from multicomponent solid dispersions. *Pharm Res.* 2017;34:990-1001.
31. Woertz K, Tissen C, Kleinebudde P, Breitkreutz J. Taste sensing systems (electronic tongues) for pharmaceutical applications. *Int J Pharm.* 2011;417:256-271.
32. Maniruzzaman M, Douroumis D. An in-vitro-in-vivo taste assessment of bitter drug: comparative electronic tongues study. *J Pharm Pharmacol.* 2015;67:43-55.
33. Shamma R, Elkasabgy N. Design of freeze-dried Soluplus/polyvinyl alcohol-based film for the oral delivery of an insoluble drug for the pediatric use. *Drug Deliv.* 2016;23:489-499.
34. Tanida S, Kurokawa T, Sato H, Kadota K, Tozuka Y. Evaluation of the micellization mechanism of an amphipathic graft copolymer with enhanced solubility of ipriflavone. *Chem Pharm Bull.* 2016;64:68-72.